# SUBSURFACE STRUCTURE INTERPRETATION OF THE NORTH OF THE WESTERN CORDILLERA, ECUADOR: INSIGHTS FROM AEROMAGNETIC DATA

Andres Carranco[1], Chris Green[2], Hernan Ugalde[3]

[1] School of Mines, Escuela Superior Politécnica de Chimborazo, Macas, EC140101, Ecuador
[2] School of Earth and Environment, University of Leeds, Leeds, LS2 9JT, United Kingdom
[3] Department of Earth Sciences, Brock University, St. Catharines, ON L2S 3A1, Canada

THE GEOLOGICAL SOCIETY OF AMERICA® CONNECTS 2021 10–13 October Portland, Oregon, USA

## 1. Introduction

The Ecuadorian Andes, located in the north of South America, comprise the Western and Easter (Real) cordilleras. The Western Cordillera possess high potential for mineral exploration due to the occurrence of volcanogenic massive sulphide (VMS), porphyry and epithermal deposits related to the Tertiary volcanism and magmatism (PRODEMINCA, 2000). This study aims to achieve a better understanding of the subsurface structure of the Western Cordillera of Ecuador between 0° and 1° N using aeromagnetic data (**Figure 1**). Specifically, this research will focus on: (1). Understanding the regional compressional tectonics that were responsible for the basement uplift and exhumation in this area. (2). Analysing the implications of the structural framework for mineral exploration in order to provide guidance for new exploration programmes.

The Northern Andes are different from the rest of the Andean orogenic belt because of the presence of mafic oceanic rocks forming the basement of the coastal forearc and western Andean regions of Ecuador and Colombia (Vallejo et al., 2019). The lithostratigraphy of the study area comprises mainly ocean floor (*high magnetic*), island arc (*mid magnetic*), continental and marine sedimentary rocks (*non-magnetic*). This sequence is covered to the west (forearc) and east (backarc) by Tertiary to present sedimentary rocks (*non-magnetic*) and continental active volcanoes (*high-mid magnetic*) respectively. Furthermore, it is affected by multiple intrusive rocks (*low-high mag*). Structurally, transcurrent faults have been reported limiting blocks and juxtaposing similar volcano-sedimentary rocks of different ages within the Western Cordillera (Vallejo et al., 2009).

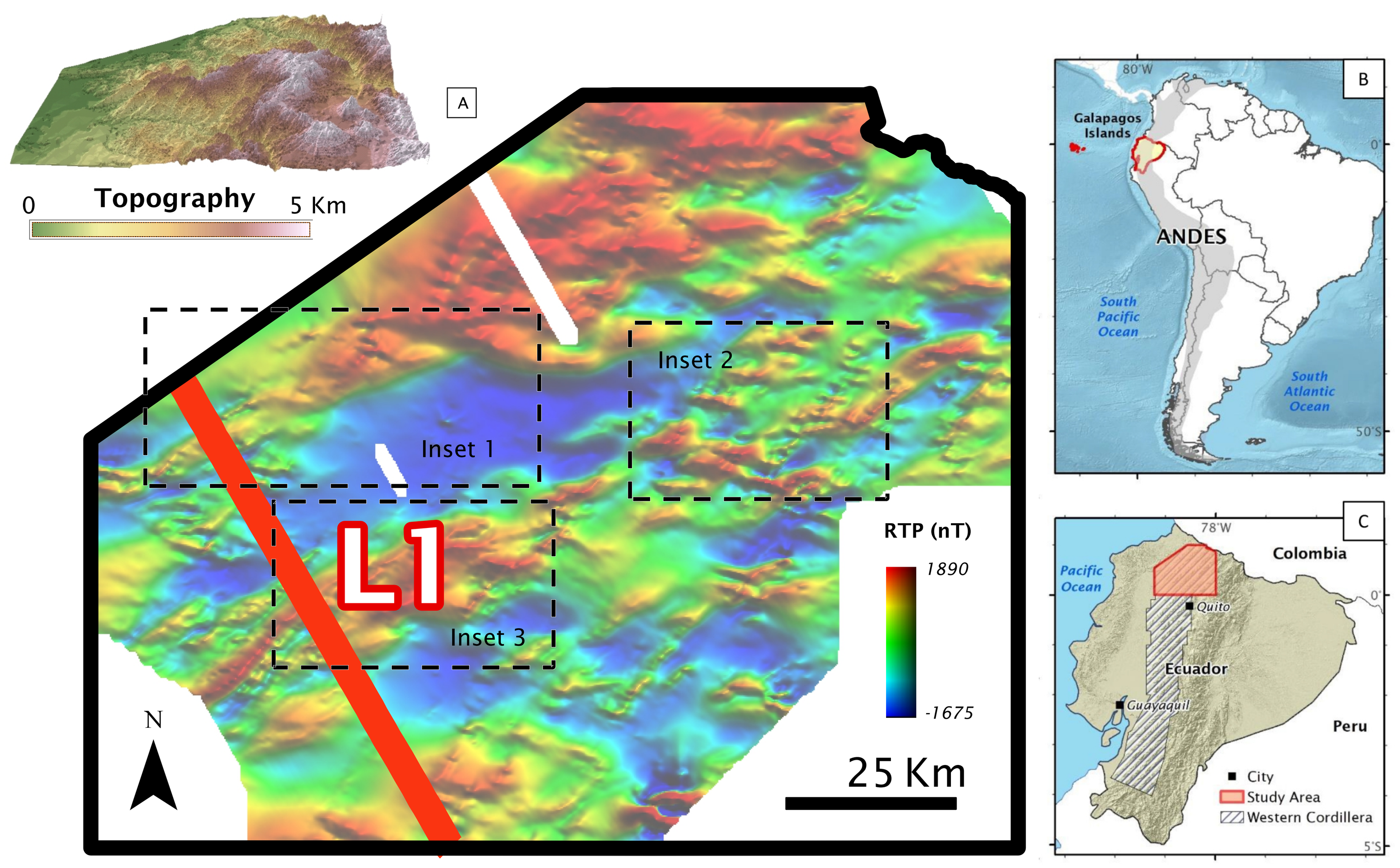


Figure 1. (A) Reduced-to-pole (RTP) magnetic anomaly map. Location of profile L1 and inset maps used for Worming are shown. Topography is included on top. (B, C) location maps of the study area.

## 2. Data and Methods

The acquisition of the aeromagnetic data was realized by the PRODEMINCA project in 1999-2000, using line spacing of 1 Km (oriented N150ºE) with control lines every 10 Km. The flight height over the study area ranges from 420-4990 meters above sea level (MASL) as the topography varies from 19 (West) to 4650 (East) MASL. Therefore, the mean flight height was about 800 m loose drape elevation. The present study has reprocessed and interpreted these data, following multiple strategies and methodologies for data enhancement, qualitative and quantitative interpretation (including 2D modelling), and structural and geophysical analysis of magnetic data. These methods and workflow are summarized in **Figure 2**.

The transformations and corrections were applied using the following parameters: Inclination: 23.12º; Declination: -0.57º and Field Strength: 30698 nT. These values were calculated by IGRF (Geosoft GM-SYS) for 0ºN latitude and 79ºW longitude, elevation 1550 MASL, on the 07/08/1999. Depth estimation was approached using three main different methods: tilt depth, local wavenumber and spectral analysis (regional). The depths were calculated using Structural index (SI) N=0, assuming a vertical contact model as it is expected in an uplifted area. 2D profile modelling was carried out using GM-SYS (Geosoft) to test and assess the interpretations. The magnetic susceptibility values reported by USGS (2003) were employed as a reference on these models because they seem consistent with the lithology reported in the study area.

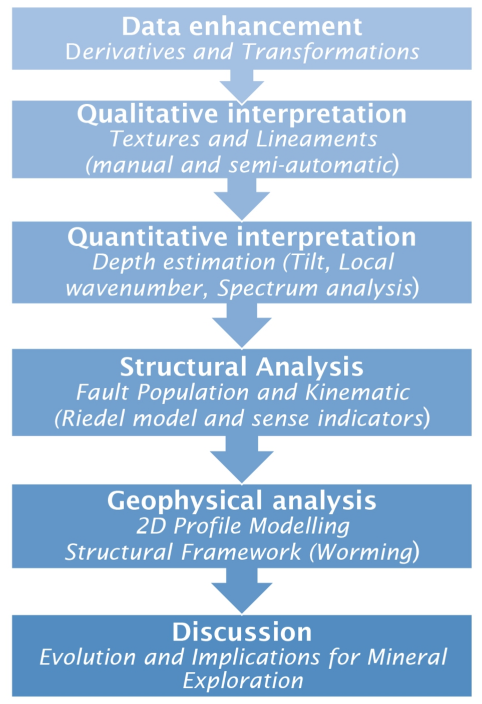


Figure 2. Workflow adapted from Ali et al. (2017) and written communications from Fairhead D. and Isles D.

## 3. Results

Four main different textures (**Figure 3**) can be identified along the study area using multiple derivatives and transformations. (1). *Chaotic* texture has been interpreted as intermediate to mafic igneous rocks. (2). *Linear* texture presents similar response to the oceanic floor, possibly associated with the mafic basement reported in the area. (3). The *smooth* texture is typically associated with sedimentary rocks, and (4). The *radial* texture is produced by active volcanoes in the area. These tonal contrasts allowed to define 13 sub-blocks based on their textural characteristics. Moreover, in total, 1495 manual and 1065 semi-automatic lineaments have been interpreted as geological structures.

Additionally, 195 local measurements show depth ranges between 0.2 and 2 Km (tilt) and between 0.3 and 5 Km (local wavenumber) (**Figure 5A,B**). Comparing both techniques, they correlate relatively well (up to ±20%) at shallow. However, the depth estimations greater than ~1500 m have more discrepancy (up to ±40%), which is expected since the methods are different. A depth solution is proposed using values where differences between the two techniques are within 10%. Furthermore, 2D modelling shows that apparently deeper sources (Local wavenumber) provide a stronger correlation between the calculated and observed magnetic anomalies (**Figure 5C**).

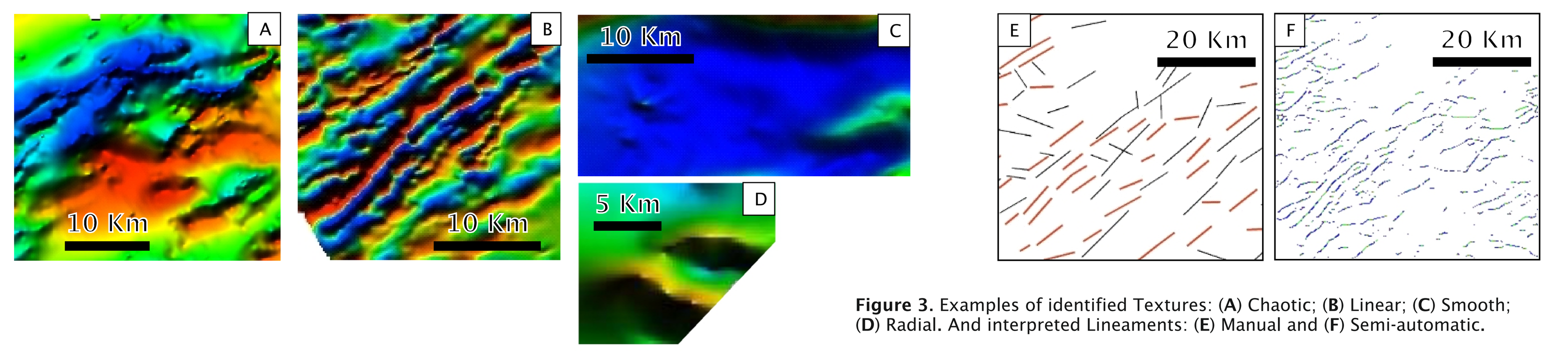


Figure 3. Examples of identified Textures: (A) Chaotic; (B) Linear; (C) Smooth; (D) Radial. And interpreted Lineaments: (E) Manual and (F) Semi-automatic.

## 4. Structural Analysis

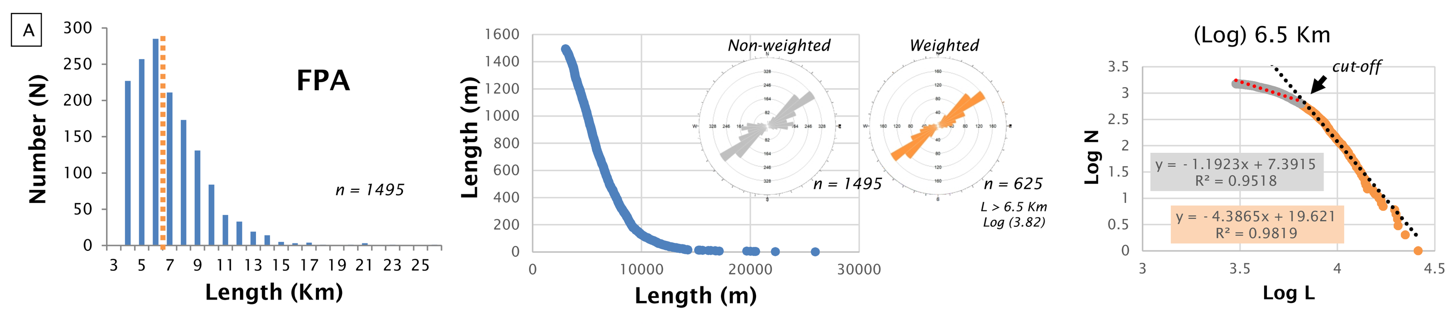


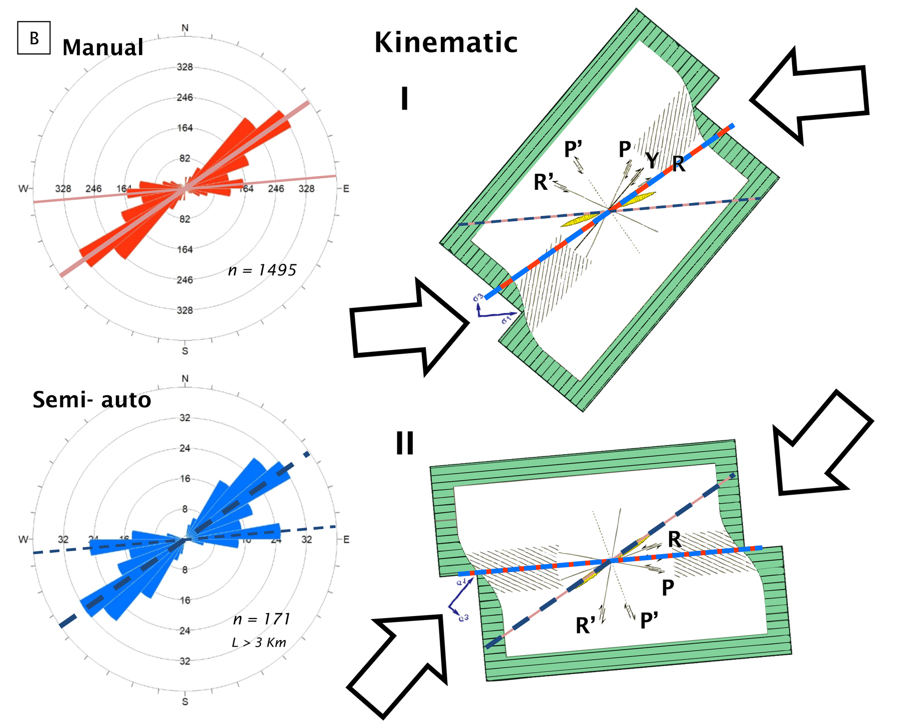


Figure 4. (A) Fault population analysis (FPA) and regression for size frequency of manual lineaments. (B) Comparison between manual and semi-automatic orientations and kinematic analysis using Riedel model (Burg, 2017)

The fault population analysis (FPA) from the interpreted lineaments shows a clear cut-off between 6 and 7 Km lengths, and the length-size distribution follows a power-law relationship (**Figure 4A**). Therefore, this relationship fits or correlates better using double power law with a 6.5 Km limit. Therefore, this cut-off could indicate the limit between small and large populations as this difference is also observed on the orientations of the lineaments.

Two principal trends were observed in both, manual and semi-automatic lineaments: a predominant NE-SW (N~55ºE) and a second mainly E-W (N~85ºE) orientations. The kinematic has been interpreted by shear-sense indicators and Riedel model. Then, apparently, (I) the dominant NE-SW trend (R shear) are mainly dextral shears caused by almost E-W compression. While (II) the E-W structures could be (a) clockwise rotation or (b) linkage of the same dextral faults, outlining that this linkage could be dextral-normal or/and sinistral-reverse faults. These sinistral faults, ideally, may be the simple shear component of compression probably caused by pure shear of two sub-blocks of the dextral strike-slip faults in direction NE-SW (Y shears) (**Figure 4B**).

## 5. Discussion

This study proposes a redefinition of the geometry and characteristics of three main system faults (WSF, CSF and ESF). They have been interpreted as isolated fault segments, except the CSF, as they are imaged discontinuous (**Figure 6A**). Moreover, the power law relationship observed on FPA suggests that the strain is distributed mainly in a few structures preferably larger than 6-7 Km, which are predominantly dextral oriented NE-SW. Conversely, the CSF presents a more complex geometry, and seems to be continuous along the area possibly because of the linkage of many segments (fault network evolution). As the displacement is related to the length, probably this system (CSF) presents higher displacement. Thus, it is possibly deeper than the other systems.

The Worming method suggests these system faults are sub-vertical based on the asymmetry of the anomalies (**Figure 6B**). It coincides with the Riedel model interpretation as it was suggested that almost NW-SE structures (R' or P' shears) may be the simple shear sinistral-reverse fault product of the main dextral faults. This deformation is common in a transpressional regime (**Figure 6C**).

Furthermore, depth estimation shows the deeper estimates coincide with the smooth texture interpreted as sediments (Sed), suggesting the presence of sub-basins. Apparently, the shape of these sub-basins is defined by the system faults. Therefore, considering the kinematic suggested by Riedel model and worms, it is proposed these structures are pull-apart sub-basins, about 2-3 km depth, according with quantitative interpretation.

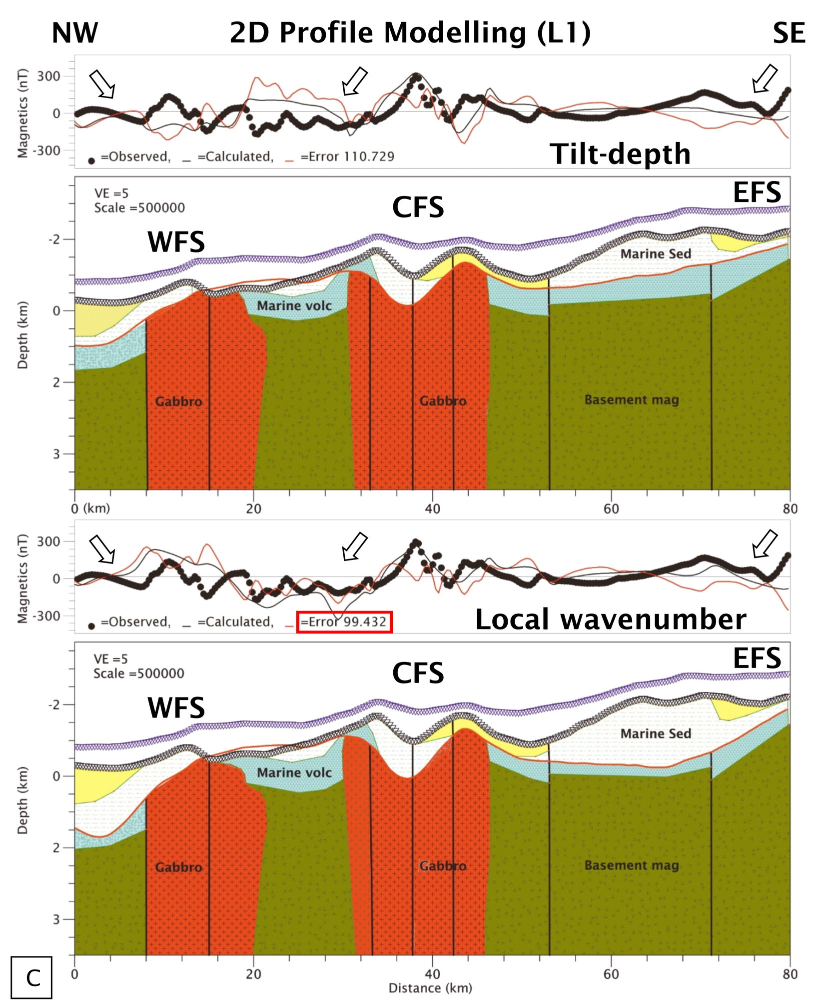


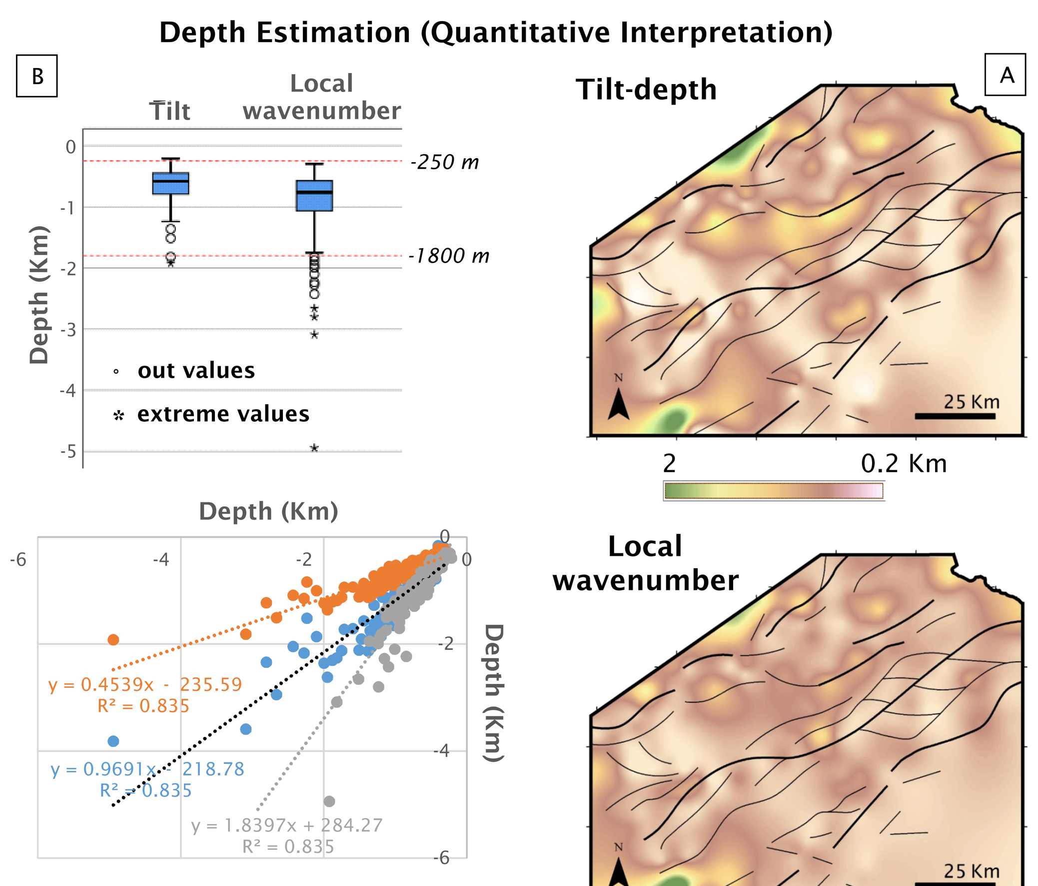


Figure 5. (A) Depth estimation to the shallowest source using Tilt and Local wavenumber (LW). (B) dispersion (boxplots) and regression analysis (LW-Tilt, Tilt-LW and Solution). (C) 2D profile modelling suggests deeper (LW) solutions.

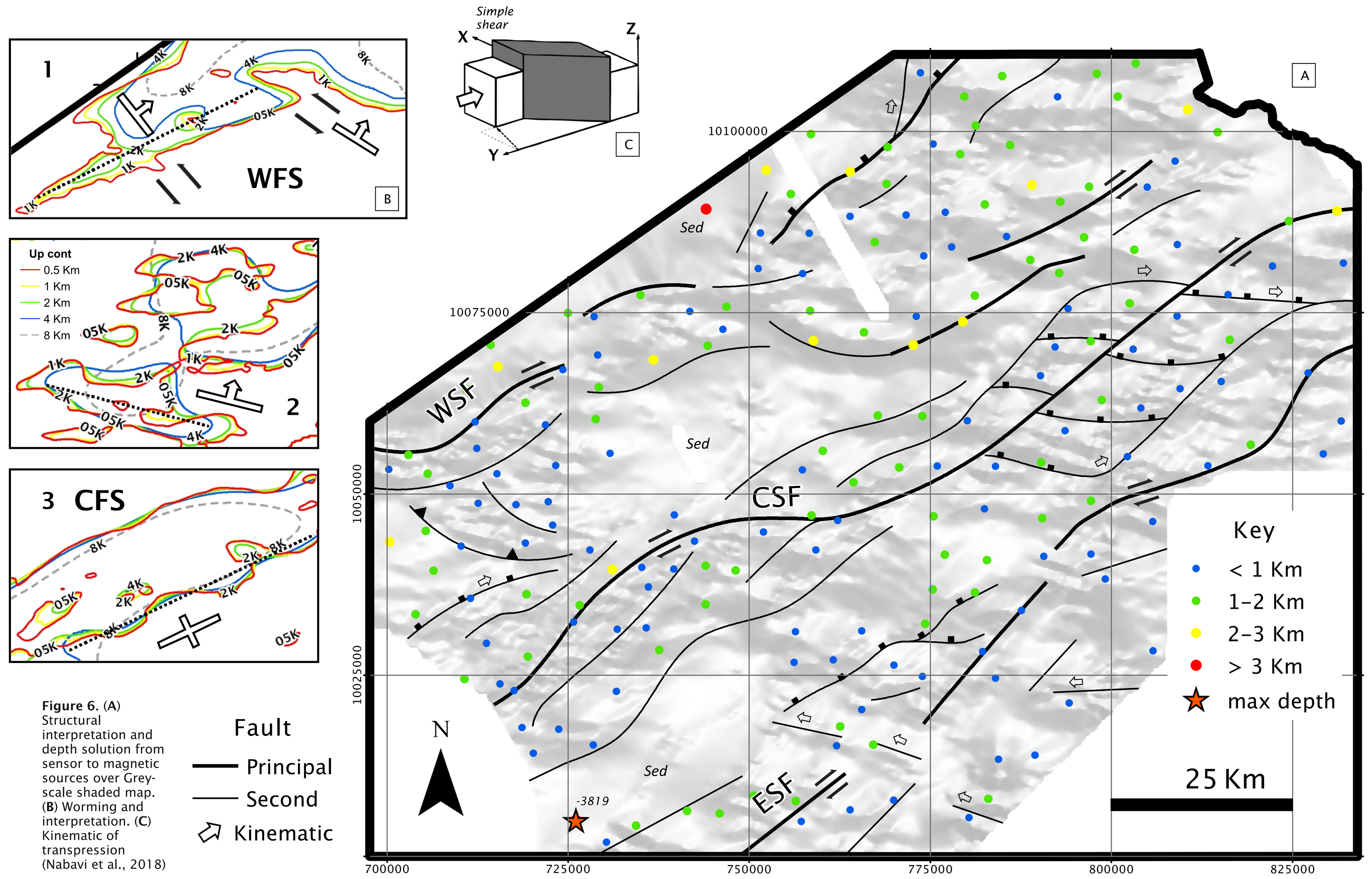


Figure 6. (A) Structural interpretation and depth solution from sensor to magnetic sources over Grey-scale shaded map. (B) Worming and interpretation. (C) Kinematic of transpression (Nabavi et al., 2018)

Consequently, a simple interpretation of the evolution may suggest that crustal fragmentation occurred during the emplacement of the basement on this region (**Figure 7B**). This probably caused a mosaic of lens shaped basement fragments bound by faults. These faults had been initially dextral-normal (transtension?), allowing space for sedimentation in the sub-basins. This theory seems to be supported by regional, novel 2D gravity and magnetic forward models and seismic data (Aizprua et al., 2020). In the case of deep faults, apparently like the CSF, this process may have even controlled the emplacement of igneous intrusions because of the thinning of the crust that allowed the heat flow to rise. Then, the current transpressional regime could have produced inversion in some of these structures, generating the basement uplift on this area.

Moreover, these system faults may have played an important role pre, syn and post mineralization on this area. First, the interaction between these structures (mainly along their tips) produces dilatation zones (**Figure 7C**), which are ideal places to host mineralization due to the local enhancement of porosity and permeability. Likewise, these regional shear zones are potential fluid pathways to magmas. In fact, deeper faults imply potential to allow multi-phase fluids transport mineralization rich in base metals from crustal or mantle levels. Finally, these fault systems are responsible for the preservation or erosion of the mineral deposits depending on the evolution of these structures along the time. Therefore, all these considerations provide simple explanations of why the structural framework, subsurface structure (**Figure 7A**) and evolution on this region, are favorable for mineral exploration.

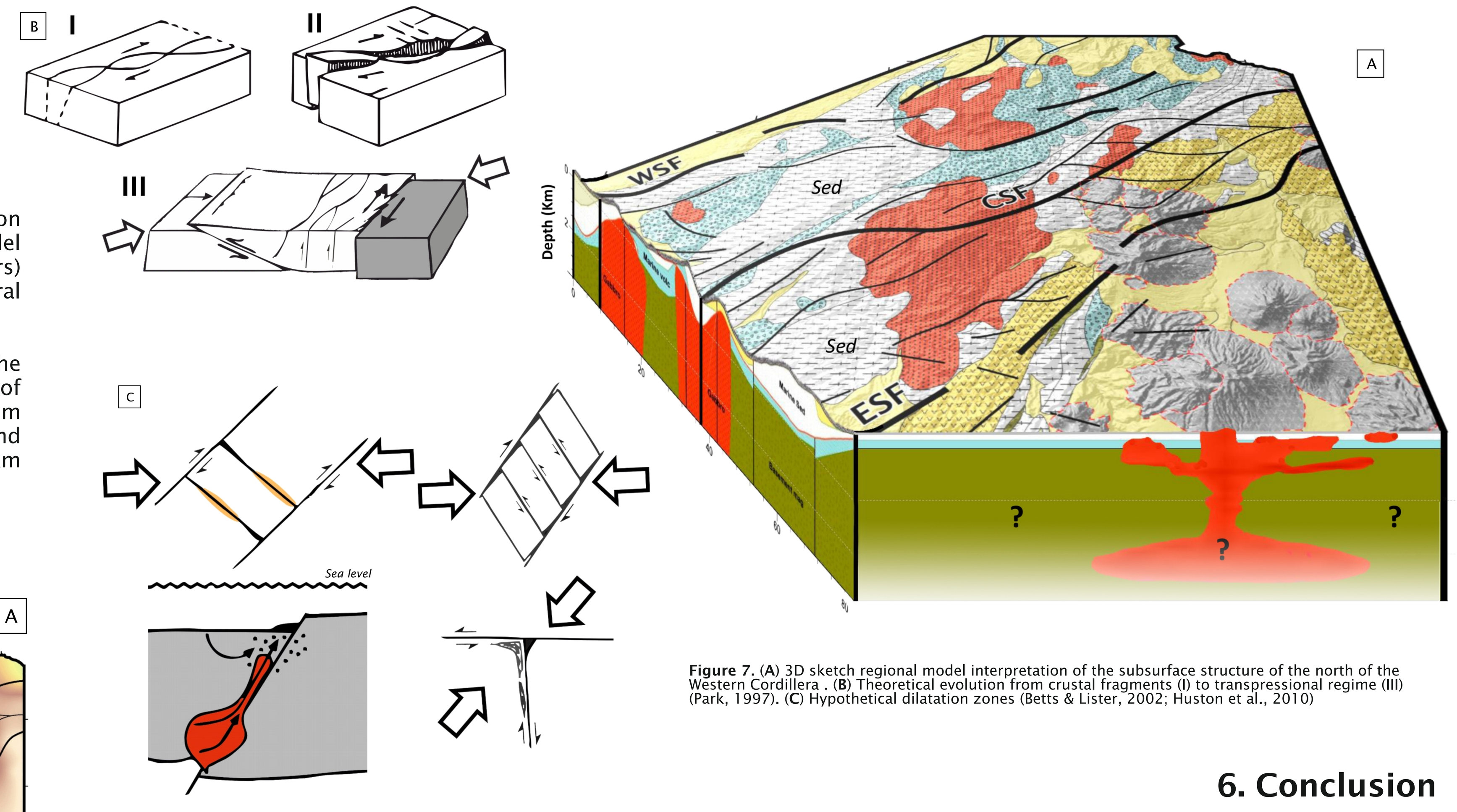


Figure 7. (A) 3D sketch regional model interpretation of the subsurface structure of the north of the Western Cordillera . (B) Theoretical evolution from crustal fragments (I) to transpressional regime (III) (Park, 1997). (C) Hypothetical dilatation zones (Betts & Lister, 2002; Huston et al., 2010)

## 6. Conclusion

Aeromagnetic data have been employed on this study as a potential tool to explore the subsurface due to the capacity to detect changes in the magnetisation of rocks, even below nonmagnetic cover (mostly recent sediments). The use of a number of interpretation techniques, including structural and geophysical analysis, have helped to redefine three main system faults (WSF, CSF and ESF) and identify deep sub-basins (to be about 2-3 Km depth). Our results support the idea of a single deformation history marked by dextral movements that were and are responsible for the current basement architecture, uplifted by transpression. Some implications of this structural setting on mineral exploration (e.g. dilatation zones, deep faults and controls, etc.) are discussed as well. Finally, although our model should be constrained or integrated with other relevant data (e.g. seismic, borehole, etc.) to assess and reduce the uncertain of this interpretation, the systematic workflow presented has allowed to diminish the ambiguity in magnetic data and obtain a better understanding of the geology and structures within the study area.

### Acknowledgements

This research was carried out as part of an MSc funded by the Chevening Scholarships and partially by the University of Leeds. The participation on GSA Connects 2021 was supported by GIRMI (Grupo de Investigación de Recursos Mineros e Ingeniería), part of the ESPOCH. We acknowledge IIGE (Instituto de Investigacion Geologico y Energetico) for providing data. Thanks go out to Dr Martin Litherland for the encouragement to explore the Ecuadorian Andes, friendship and tips on scientific writing.

### References

- Aizprua, C., Witt, C., Brönner, M., Johansen, S. E., Barba, D., Hernandez, M. J. (2020). Forearc Crustal Structure of Ecuador Revealed by Gravity and Aeromagnetic Anomalies and Their Geodynamic Implications. Lithosphere; 2020 (1): 2810692.
- Ali, M., Fairhead , J., Green, C. and Noufal , A. (2017). Basement structure of the United Arab Emirates derived from an analysis of regional gravity and aeromagnetic database. Tectonophysics, 712 713, pp.503 522.
- Betts, P. and Lister, G. (2002). Geodynamically indicated targeting strategy for shale - hosted massive sulfide Pb – Zn – Ag mineralisation in the Western Fold Belt, Mt Isa terrane. Australian Journal of Earth Sciences, 49(6), pp.985-1010.
- Burg, J. (2017). Strike-slip and oblique-slip tectonics.
- Huston, D., Pehrsson, S., Eglington, B. and Zaw, K. (2010). The Geology and Metallogeny of Volcanic-Hosted Massive Sulfide Deposits: Variations through Geologic Time and with Tectonic Setting. Economic Geology, 105(3), pp.571-591.
- Nabavi, S., Alavi, S., Mohammadi, S. and Ghassemi, M. (2018). Mechanical evolution of transpression zones affected by fault interactions: Insights from 3D elasto-plastic finite element models. Journal of Structural Geology, 106, pp.19-40.
- Park, R. (1997). Foundations of structural geology.
- PRODEMINCA (2000). Manual of exploration of metalliferous deposits in Ecuador. Quito: UCP Prodeminca Proyecto.
- USGS (2003). Density and magnetic suseptibility values for rocks in the Talkeetna Mountains and adjacent region, south-central Alaska. Report.
- Vallejo, C., Spikings, R., Horton, B., Luzieux, L., Romero, C., Winkler, W. and Thomsen, T. (2019). Late Cretaceous to Miocene stratigraphy and provenance of the Coastal Forearc and Western Cordillera of Ecuador: Evidence for accretion of a single oceanic Plateau. In: B. Horton and A. Folguera, ed., Andean Tectonics, 1st ed. Elsevier.

Correspondence should be addressed to carranco.lopez.andres@gmail.com